Mechanical Systems and Signal Processing 222 (2025) 111768

Contents lists available at ScienceDirect

Mechanical Systems and Signal Processing

journal homepage: www.elsevier.com/locate/ymssp

An efficient Bayesian updating framework for characterizing the posterior failure probability

Pei-Pei Li [a,*], Yan-Gang Zhao [b], Chao Dang [a], Matteo Broggi [c], Marcos A. Valdebenito [a], Matthias G.R. Faes [a]

[a] Chair for Reliability Engineering, TU Dortmund University, Leonhard-Euler-Straße 5, 44227 Dortmund, Germany
[b] Key Laboratory of Urban Security and Disaster Engineering of Ministry of Education, Beijing University of Technology, Beijing 100124, China
[c] Institute for Risk and Reliability, Leibniz University Hannover, Callinstr. 34, Hannover 30167, Germany

ARTICLE INFO

Communicated by John E. Mottershead

Keywords:
Bayesian updating
Posterior failure probability
Sparse grid numerical integration
Shifted lognormal distribution

ABSTRACT

Bayesian updating plays an important role in reducing epistemic uncertainty and making more reliable predictions of the structural failure probability. In this context, it should be noted that the posterior failure probability conditional on the updated uncertain parameters becomes a random variable itself. Hence, characterizing the statistical properties of the posterior failure probability is important, yet challenging task for risk-based decision-making. In this study, an efficient framework is proposed to fully characterize the statistical properties of the posterior failure probability. The framework is based on the concept of Bayesian updating and keeps the effect of aleatory and epistemic uncertainty separated. To improve the efficiency of the proposed framework, a weighted sparse grid numerical integration is suggested to evaluate the first three raw moments of the corresponding posterior reliability index. This enables the reuse of evaluation results stemming from previous analyses. In addition, the proposed framework employs the shifted lognormal distribution to approximate the probability distribution of the posterior reliability index, from which the mean, quantile, and even the distribution of the posterior failure probability can be easily obtained in closed form. Four examples illustrate the efficiency and accuracy of the proposed method, and results generated with Markov Chain Monte Carlo combined with plain Monte Carlo simulation are employed as a reference.

1. Introduction

Uncertainties pervade nearly all engineering problems, arising from factors such as incomplete knowledge or experimental data, modeling assumptions, measuring errors, environmental effects, and more [1–3]. Regarding engineering purposes, these uncertainties can be broadly categorized into two main types: aleatory uncertainty and epistemic uncertainty [4–7]. To rationally address these uncertainties, many scholars have focused on developing and applying a probabilistic framework to quantify aleatory and epistemic uncertainties [8–11]. Within this probabilistic framework, aleatory uncertainty is generally represented by either a probability density function (PDF) or a cumulative distribution function (CDF) [12]. In addition, epistemic uncertainty represents a lack of knowledge which, in principle, can be reduced whenever additional information becomes available [9].

Recently, due to the advancements in monitoring and sensor technology [13], data coming from inspections or measurements

* Corresponding author.
E-mail address: li.peipei@tu-dortmund.de (P.-P. Li).

https://doi.org/10.1016/j.ymssp.2024.111768
Received 23 January 2024; Received in revised form 26 May 2024; Accepted 22 July 2024
Available online 6 August 2024

allows collecting relevant information about structural parameters or responses. This creates favorable conditions for reducing epistemic uncertainties. Bayesian inference is an appropriate method for incorporating data measurements into the probabilistic model [14,15], as it ensures consistent treatment of uncertainty and enhances the plausibility of failure probability analysis [16–20]. Therefore, based on Bayesian theory, additional data, for instance coming from measurements, can be used to reduce epistemic uncertainty in practical engineering applications, leading to a "posterior" failure probability [21,22]. Indeed, the term "posterior" reflects the fact that the effect of additional data is assimilated into the failure probability associated with a structural model. As such, these data enhance the accuracy of probabilistic estimates for structural failure probabilities in a logical manner, ultimately boosting our confidence in predicting future structural performance and facilitating more efficient, risk-based decision-making [23,24].

Aimed at evaluating the expected value of posterior failure probability (usually termed as "robust posterior failure probability") with the aid of the concept of Bayesian updating has been an active topic for developments in last years. For instance, Der Kiureghian [4] employed the Bayesian method to combine data measurements and reliability analysis, deriving the posterior distribution of uncertain parameters through the conjugate prior distribution, and then obtaining the expected value of posterior failure probability. Beck and Au [17] proposed an adaptive Markov chain Monte Carlo simulation method to evaluate the expected value of posterior failure probability based on the Metropolis-Hasting algorithm and a concept similar to simulated annealing. Papadimitriou et al. [25] presented a general framework to update the robust failure probability using the theorem of total probability, which is the probabilistic integral of the failure probabilities conditional on the given parameters. Jensen et al. [26] proposed a method for updating robust failure probability that involves updating the uncertain parameters using the transitional Markov chain Monte Carlo simulation method and then, using the updated distribution of these uncertain parameters to calculate a robust failure probability. Straub et al. [27] developed the Bayesian Updating with Structural Reliability method (BUS) [28] to obtain the posterior failure probability without the need for posterior samples of uncertain parameters, and Liu et al. [29] then utilized this method to calculate the robust updated failure probability. Fan et al. [30] extended the probability density evolution method to determine the robust posterior failure probability based on data measurements of deteriorating structures. Li et al. [31] proposed an efficient method to directly assess the expected value of the posterior failure probability considering the structural deterioration, which avoids the necessity for iterative reliability analyses.

The approaches for updating described previously focus on the expected value to characterize the posterior failure probability. However, focusing exclusively on updating the expected value of the failure probability, encapsulating both the aleatory uncertainty and epistemic uncertainty together, may be insufficient to make efficient and unbiased decisions. To provide a rational method for fully characterizing the posterior failure probability, some methods have been proposed. A common method is to employ the Monte Carlo simulation method (MCS) [32] to sample the posterior failure probability, employing samples conditional on the updated uncertain parameters after determining posterior distributions of these parameters, and then obtain the quantity of interest. However, it often comes with a substantial cost because it requires a large number of posterior failure probability samples to obtain sufficiently accurate results and cannot be given in an explicit expression. To address these drawbacks, several approximate methods have been introduced. Papadimitriou et al. [25] developed a novel technique based on Laplace's method for asymptotic approximation to fit the posterior failure probability when the probabilities of failure conditional on the uncertain parameters are available. Then, Der Kiureghian and Ditlevsen [5] derived an explicit expression of posterior failure probability conditional on the updated distribution parameters when their explicit PDFs are accessible through the first-order approximation approach. However, those approximate methods are applicable to a certain range of engineering problems and may not produce probability quantiles, and can be time-consuming when multiple updates are required. In summary, most existing studies may not be able to provide an efficient and broadly applicable method to fully characterize the posterior failure probability based on the concept of Bayesian updating, including their quantiles and probabilistic properties. Therefore, it is of great significance to establish a rational and efficient framework for fully describing the posterior failure probability.

In this study, an efficient framework for completely characterizing the posterior failure probability based on the concept of Bayesian updating is established. It is assumed that epistemic uncertainties appear in the characterization of distribution parameters associated with the characterization of aleatory uncertainty. The proposed method uses the shifted lognormal distribution [33,34] to model the distribution of the posterior reliability index. Based on the computational relationship between the posterior failure probability and the posterior reliability index, the mean, quantile, and even probability distribution of the posterior failure probability can be readily obtained utilizing the probability distribution of the posterior reliability index. In addition, a weighted sparse grid algorithm [35] and information reuse [31] are employed to assess the statistical moments of the posterior reliability index, which enables the proposed method to avoid repeated reliability analyses conditional on distribution parameters or re-assess the posterior samples for each update.

The structure of this paper is as follows. In Section 2, the reliability updating problem considered in the present study is formulated. In Section 3, an efficient method for completely characterizing the posterior failure probability based on the concept of Bayesian updating is proposed. Section 4 describes four numerical examples to demonstrate the efficiency and effectiveness of the proposed method, using the results obtained from Monte Carlo Markov Chain (MCMC) [17] combined with Monte Carlo simulation (MCS) as the benchmark for comparison. In Section 5, the main conclusions of this study are summarized.

2. Problem statement

Consider a numerical model of the structure, which is dependent on the basic random variable vector $\mathbf{X}$. The behavior of this model is characterized through a so-called performance function $G(\mathbf{X})$. This function is defined such that $G(\mathbf{X}) \leq 0$ whenever a particular combination of the basic random variable vector $\mathbf{X}$ leads to undesirable behavior of the structure. It is further assumed that the

probability model associated with $\mathbf{X}$ contains epistemic uncertainty, which is reflected in distribution parameters that are represented by the vector $\boldsymbol{\Theta}$ with probability distribution $f_{\boldsymbol{\Theta}}(\boldsymbol{\theta})$. Then, the PDF of $\mathbf{X}$ can be modeled through a vector $\mathbf{X}$ of basic random variables with probability density $f_{\mathbf{X}}(\mathbf{x}|\boldsymbol{\theta})$. Considering all definitions discussed previously, the probability that the structure undergoes an undesirable behavior (which is termed as the "failure probability") can be expressed in terms of the following probability integral [4]:

$$P_f(\boldsymbol{\theta}) = \int_{G(\mathbf{X})\leqslant 0} f_{\mathbf{X}}(\mathbf{x}|\boldsymbol{\theta})d\mathbf{x}, \tag{1}$$

where $P_f(\boldsymbol{\theta})$ represents the failure probability conditional on the distribution parameter vector $\boldsymbol{\theta}$, and the corresponding reliability index can be given as:

$$\beta(\boldsymbol{\theta}) = \Phi^{-1}\left[1 - P_f(\boldsymbol{\theta})\right], \tag{2}$$

where $\Phi^{-1}[\cdot]$ indicates the inverse of the standard normal CDF.

It should be noted in Eq. (2) that the reliability index calculated from the failure probability is referred to as the generalized reliability index. This reliability index can be obtained regardless of whether the performance function conforms to a normal distribution. In addition, in this equation both $P_f(\boldsymbol{\theta})$ and $\beta(\boldsymbol{\theta})$ are uncertain because they depend on the distribution parameter vector $\boldsymbol{\theta}$. Thus, both the failure probability and reliability index can be termed as random variables and evaluated in a probabilistic manner.

The definition of the failure probability and associated reliability index is presented in Eqs. (1) and (2) correspond to the situation when aleatory uncertainty and epistemic uncertainty coexist. In practice, data measurements of the physical random properties (denoted as $D_{\mathbf{X}}$) can be readily obtained through various methods. These data measurements can then be used to reduce the epistemic uncertainty associated with the distribution parameters. This process naturally falls within the framework of hierarchical Bayesian model updating [36]. Thus, following the concept of Bayesian updating [14], it is possible to update the state of knowledge regarding the distribution parameters $\boldsymbol{\theta}$ by means of:

$$f'_{\boldsymbol{\Theta}}(\boldsymbol{\theta}|D_{\mathbf{X}}) = kL(D_{\mathbf{X}}|\boldsymbol{\theta})f_{\boldsymbol{\Theta}}(\boldsymbol{\theta}), \tag{3}$$

where $f_{\boldsymbol{\Theta}}(\boldsymbol{\theta})$ represents the initial ("prior") PDF of distribution parameters, which reflects the current state of knowledge with respect to $\boldsymbol{\theta}$; $f'_{\boldsymbol{\Theta}}(\boldsymbol{\theta}|D_{\mathbf{X}})$ represents the updated ("posterior") PDF associated with the distribution parameters, which includes the newly acquired data measurements $D_{\mathbf{X}}$; $L(D_{\mathbf{X}}|\boldsymbol{\theta})$ represents the likelihood function of the data measurements; and k represents the Bayesian evidence, which can be formulated as follows:

$$k = \left[\int_{-\infty}^{\infty} L(D_{\mathbf{X}}|\boldsymbol{\theta})f_{\boldsymbol{\Theta}}(\boldsymbol{\theta})\mathrm{d}\boldsymbol{\theta}\right]^{-1}. \tag{4}$$

For each set of the data measurements of the random variables $\mathbf{X}$, represented as $D_{\mathbf{X}i}$, where $i = 1, 2, \ldots, N_d$, the likelihood function in Eqs. (3)-(4) can be formulated as

$$L\left(D_{\mathbf{X}_i}\middle|\boldsymbol{\theta}\right) \propto Pr\left(D_{\mathbf{X}_i}\middle|\boldsymbol{\Theta} = \boldsymbol{\theta}\right), \tag{5}$$

where $\Pr(\cdot)$ represents the probability of an event occurring. If the data measurement samples $D\mathbf{x}_i$ are statistically independent between them conditional on $\boldsymbol{\Theta} = \boldsymbol{\theta}$, then the likelihood function can be expressed as $L(D_{\mathbf{X}_i}|\boldsymbol{\theta}) = \prod_{i=1}^{N_d} f_{\mathbf{X}|\boldsymbol{\Theta}}(D_{\mathbf{X}_i}|\boldsymbol{\theta})$.

In the case where the data measurements of the random variables $D_{\mathbf{X}i}$ are used to update the failure probability, the updated distribution parameters $\boldsymbol{\theta}^{up}$ (whose probability distribution is $f'_{\boldsymbol{\Theta}}(\boldsymbol{\theta}|D_{\mathbf{X}})$), will replace the distribution parameters $\boldsymbol{\theta}$ in Eq. (1), where the apex "up" denotes updated. Then, one can define new random variables associated with the failure probability and reliability index based on the updated distribution parameters $\boldsymbol{\theta}^{up}$, which are denoted as P_f^{up} and β^{up}. Similarly, the posterior failure probability P_f^{up} and the associated posterior reliability index β^{up} are also uncertain and can be treated as random variables. The dispersion of their associated PDFs, as quantified by their corresponding standard deviations, is a measure of the degree of imperfect knowledge (epistemic uncertainty). However, when more data measurements become available, it is expected that the dispersion will decrease.

In the context of structural risk analysis, providing a comprehensive depiction of the epistemic uncertainty associated with the posterior failure probability holds significant importance [4,5,37]. In this regard, one should pay particular attention to three critical aspects: the expected value of the posterior failure probability, the quantiles of the posterior failure probability, and the probability distribution of the posterior failure probability.

According to the theorem of total probability, the expected value of the posterior failure probability $\overline{P_f^{up}}$ can be calculated considering the definition of failure probability as cast in Eq. (1) together with the posterior PDF $f'_{\boldsymbol{\Theta}}(\boldsymbol{\theta}|D_{\mathbf{X}})$ as shown in Eq. (3), leading to:

$$\overline{P_f^{up}} = E\left[P_f^{up}\right] = \int P_f(\boldsymbol{\theta})f'_{\boldsymbol{\Theta}}(\boldsymbol{\theta}|D_{\mathbf{X}})d\boldsymbol{\theta}, \tag{6}$$

where $E[\cdot]$ denotes the expectation value.

To calculate Eq. (6), commonly used methods are to use the obtained posterior samples of distribution parameters to conduct the corresponding reliability analysis. In the case of multiple updates (that is, when the set of data measurements grows over time), such

procedure can become time-consuming, as it needs to consider new posterior samples of distribution parameters and to repeat the corresponding reliability analysis. Furthermore, simply obtaining the expected value of posterior failure probability encapsulates both aleatory and epistemic uncertainty together in a single quantity, which may be often insufficient for risk-based decision-making, while a complete characterization of posterior failure probability remains a challenging issue. In view of this problem, the reminder of this contribution establishes an efficient framework to completely characterize the probabilistic characteristic of the posterior failure probability. Such an approach proves to be most convenient, as it keeps the different sources of uncertainty (aleatory and epistemic) separated.

3. Proposed method for completely characterizing the posterior failure probability

To comprehensively depict the probabilistic characteristics of the posterior failure probability, one of the primary objectives is to obtain the probability distribution of the posterior failure probability. However, the focus of this study is not to directly approximate the probability distribution of posterior failure probability itself, but to first fit the probability distribution of the corresponding posterior reliability index based on the shifted lognormal distribution, which may be simpler to analyze [33,34]. The basic concepts and steps of this section are as follows: In section 3.1, the first three moments of the posterior reliability index are calculated using a sparse grid numerical integration (SGNI) strategy [35]. In section 3.2, the PDF and CDF of the posterior reliability index are approximated based on the shifted lognormal distribution. In section 3.3, the mean, quantiles, and probability distribution of the posterior failure probability are derived by considering the probability distribution of the associated posterior reliability index.

3.1. First three moments of the posterior reliability index

By definition, the l-th raw moment of the posterior reliability index can be formulated as follows [38]:

$$\hbar_{lB} = \int_{\boldsymbol{\theta}} [\beta(\boldsymbol{\theta})]^l f'_{\boldsymbol{\Theta}}(\boldsymbol{\theta}|D_{\mathbf{X}})d\boldsymbol{\theta}. \tag{7}$$

The posterior distribution appearing in Eq. (7) can be expressed by the term containing the likelihood function (which is affected by updates) and the prior distribution. This leads to the so-called updating factor proposed in Li et al. [31] and thus, Eq. (7) can be reformulated as follows:

$$\hbar_{lB} = \int_{\boldsymbol{\theta}} [\beta(\boldsymbol{\theta})]^l \xi(\boldsymbol{\theta}) f_{\boldsymbol{\Theta}}(\boldsymbol{\theta})d\boldsymbol{\theta}, \tag{8}$$

where $\xi(\boldsymbol{\theta}) = kL(D_{\mathbf{X}}|\boldsymbol{\theta})$ is the updating factor, which represents the part that changes with updates; and the Bayesian evidence k needs to be calculated before $\xi(\boldsymbol{\theta})$ is determined by integrating the likelihood over the prior PDF $f_{\boldsymbol{\Theta}}(\boldsymbol{\theta})$.

From Eq. (8), it is evident that the l-th raw moment of the posterior reliability index can also be computed as the expected value of $[\beta(\boldsymbol{\theta})]^l\,\xi(\boldsymbol{\theta})$ under the prior PDF $f_{\boldsymbol{\Theta}}(\boldsymbol{\theta})$. Therefore, by integrating the function $[\beta(\boldsymbol{\theta})]^l\,\xi(\boldsymbol{\theta})$ considering the prior PDF $f_{\boldsymbol{\Theta}}(\boldsymbol{\theta})$, the l-th raw moments of the posterior reliability index can be determined. To solve Eq. (8) numerically, this study adopts the SGNI derived from the Smolyak algorithm [35,39] due to its ability to strike a favorable balance between efficiency and accuracy when evaluating statistical moments [40].

According to the SGNI derived from Smolyak algorithm [35], Eq. (8) can be calculated as:

$$\begin{aligned}\hbar_{lB} = &\sum_{\boldsymbol{i}\in H(q,N)} (-1)^{q+N-|\boldsymbol{i}|}\binom{N-1}{q+N-|\boldsymbol{i}|} \\ &\times \sum_{j_1=1}^{2^{i_1}-1}\cdots\sum_{j_N=1}^{2^{i_N}-1} \beta\left[T^{-1}(u_{j_1}),\cdots,T^{-1}(u_{j_N})\right]^l \cdot \xi\left[T^{-1}(u_{j_1}),\cdots,T^{-1}(u_{j_N})\right] p_{j_1}\cdots p_{j_N}\end{aligned}, \tag{9}$$

where $\xi\left[T^{-1}(u_{j_1}),\cdots,T^{-1}(u_{j_N})\right]$ is given as:

$$\begin{aligned}\xi\left[T^{-1}(u_{j_1}),\cdots,T^{-1}(u_{j_N})\right] &= k\cdot L\left[T^{-1}(u_{j_1}),\cdots,T^{-1}(u_{j_N})\right] \\ &= \frac{L\left[T^{-1}(u_{j_1}),\cdots,T^{-1}(u_{j_N})\right]}{\sum_{\boldsymbol{i}\in H(q,N)}(-1)^{q+N-|\boldsymbol{i}|}\binom{N-1}{q+N-|\boldsymbol{i}|}\times\sum_{j_1=1}^{2^{i_1}-1}\cdots\sum_{j_N=1}^{2^{i_N}-1}L\left[T^{-1}(u_{j_1}),\cdots,T^{-1}(u_{j_N})\right]\cdot p_{j_1}\cdots p_{j_N}},\end{aligned} \tag{10}$$

and $T^{-1}(\cdot)$ indicates the inverse normal transformation operator between the prior CDF of the distribution parameters $F_{\boldsymbol{\Theta}}(\boldsymbol{\theta})$ and the standard normal CDF $\Phi(\mathbf{u})$. Herein $\mathbf{u}$ furthermore denotes the standard normal random vector.$u_{j_h} = \sqrt{2}\xi_{j_h}$ and $p_{j_h} = \frac{1}{\sqrt{\pi}}\zeta_{j_h}(h = 1, \ldots, N)$ represent the grid points of the SGNI and their corresponding weights within the standard normal space. These weights can be determined using the Gaussian-Hermite formula related to the weight $\exp(-x^2)$. It needs to be noted that the calculation of Eq. (9) involves first calculating the Bayesian evidence k using SGNI with the same grid points, as shown in Eq. (10). $\boldsymbol{i} = (i_1,\cdots,i_N) \in \mathbb{N}_+^N$; $|\boldsymbol{i}| = i_1 + \cdots + i_N$ represents the sum of the multiple indices. The non-negative integer q represents the accuracy level, and the set $H(q, N)$ can

be represented by

$$H(q,N)=\left\{\boldsymbol{i}\in\mathbb{N}_{+}^{N},\ \boldsymbol{i}\geqslant(1,\ldots,1):q+1\leqslant\sum_{n=1}^{N}i_n\leqslant q+N\right\}. \tag{11}$$

The selection of accuracy level q can be initially chosen based on the nonlinearity of the kernel $[\beta(\boldsymbol{\theta})]^{l}\,\xi(\boldsymbol{\theta})$ in Eq. (9). For scenarios with mild nonlinearity, setting $q=1$ could suffice. However, in cases of pronounced nonlinearity, a higher exactness level, typically $q\geq 2$, is recommended [35]. Subsequently, the accuracy level q of the Smolyak-type quadrature can be adjusted according to the transmission error [41], which is required to ensure a balance between accuracy and efficiency using SGNI. It is worth noting that once the specified accuracy level q is determined, the interpolation points of each distribution parameter $\Theta_i=T^{-1}(u_i)$ $(i=1\ \ldots\ N)$ are also determined and will not change, because the prior distribution remains unchanged during the whole updating process. This implies that when dealing with multiple updates, the values of the posterior reliability index for each set of interpolation points are determined and can be recycled in subsequent updates.

Once the first three raw moments of posterior reliability index (i.e., $\hbar_{1B}$, $\hbar_{2B}$, and $\hbar_{3B}$) are determined, the first three moments of the posterior reliability index can be evaluated as follows [38,42]:

$$\mu_B=\hbar_{1B}, \tag{12}$$

$$\sigma_B=\sqrt{\hbar_{2B}-\hbar_{1B}^2}, \tag{13}$$

$$\alpha_{3B}=\left(\hbar_{3B}-3\hbar_{2B}\hbar_{1B}+2\hbar_{1B}^3\right)/\left(\sigma_B^3\right). \tag{14}$$

3.2. Probability distribution of the posterior reliability index

Upon determining the first three central moments of the posterior reliability index, i.e., mean (μ_B), standard deviation (σ_B), and skewness (σ_{3B}), the probability distribution of the posterior reliability index can be approximated through the utilization of parameterized distributions. In this study, the shifted lognormal distribution [33,34] was selected, mainly because: first, the parameters of this distribution are explicitly expressed using only its first three central moments and the quantiles of the posterior failure probability derived from this distribution are explicit and simple, which is convenient for engineering use; second, it can be found that for most problems the distribution of the posterior reliability index is well-shaped. Thus, although the shifted lognormal distribution is simple, it is still flexible enough to fit the body and tail of the posterior reliability index distribution.

For convenience, the notations $f_{\beta^{up}}(\beta)$ and $F_{\beta^{up}}(\beta)$ are introduced to represent the PDF and CDF of the posterior reliability index, respectively. Based on the shifted lognormal distribution, the PDF of the posterior reliability index can be formulated as follows

$$f_{\beta^{up}}(\beta)=\frac{1}{(\beta-\lambda)\sqrt{2\pi}\upsilon}\times\exp\left\{-\frac{1}{2\upsilon^2}[\ln(\beta-\lambda)-\zeta\,]^2\right\}, \tag{15}$$

and its CDF can be derived as:

$$F_{\beta^{up}}(\beta)=\Phi\left[\frac{\ln(\beta-\lambda)-\zeta}{\upsilon}\right], \tag{16}$$

where λ, ζ, and υ represent the distribution parameters related to location, scale, and shape respectively. The three distribution parameters for the shifted lognormal distribution λ, ζ, and υ can be readily determined by using the first three central moments of the posterior reliability index, and the relationship between them can be given as

$$\mu_B=\lambda+\exp\left(\zeta+\upsilon^2/2\right), \tag{17}$$

$$\sigma_B=\sqrt{[\exp(\upsilon^2)-1\,]\cdot\exp(2\lambda+\upsilon^2)}, \tag{18}$$

$$\alpha_{3B}=\left[\exp\left(\upsilon^2\right)+2\,\right]\sqrt{\exp(\upsilon^2)-2}. \tag{19}$$

It should be noted that when dealing with positive skewness, Eq. (15) and Eq. (16) can be directly applied. However, in the case of negative skewness, the PDF can be obtained by adopting the absolute value of the skewness and subsequently mirroring the PDF about $\beta=\mu_B$, and the CDF can also be determined accordingly [34].

3.3. Complete characterization of the posterior failure probability

In this section, a framework will be established to completely characterize the probabilistic characteristics of the posterior failure probability. This framework considers the probability distribution of the corresponding posterior reliability index to obtain the mean, quantile, and even probability distribution of the posterior failure probability.

3.3.1. Estimation of the expected value of the posterior failure probability

The PDF of the posterior reliability index is considered to evaluate the expected value of the posterior failure probability. In this sense, the expected value of the posterior failure probability given in Eq. (6) can be rewritten as:

$$\overline{P_f^{up}} = E\left[P_f^{up}\right] = \int \Phi[-\beta] \cdot f_{\beta^{up}}(\beta) d\beta. \tag{20}$$

It can be seen from Eq. (20) that once the PDF of the posterior reliability index has been determined (as shown in Eq. (15)), the solution of Eq. (20) can be regarded as a one-dimensional numerical integration problem and can be readily evaluated by direct quadrature.

3.3.2. Determination of the quantiles of the posterior failure probability

In many cases, the quantile of the posterior failure probability is also an important index for practitioners [4,37], in addition to the expected value calculated in Section 3.3.1. To obtain the quantiles of the posterior failure probability, the corresponding quantiles of the posterior reliability index need to be determined first.

Following the principle of equal probability, the relationship between the CDF of the posterior reliability index and the standard normal random variable U can be expressed as:

$$F_{\beta^{up}}(\beta) = \Phi(U). \tag{21}$$

Based on Eq. (16) and Eq. (21), the relationship between the standard normal random variable and the posterior reliability index can be deduced as

$$U = \frac{\ln(\beta - \lambda) - \zeta}{\upsilon}. \tag{22}$$

The quantiles of the posterior reliability index with confidence level α (denoted as β_α^{up}) can be represented as follows:

$$F_{\beta^{up}}\left[\beta_\alpha^{up}\right] = \Phi(U) = \alpha. \tag{23}$$

According to Eq. (22) and Eq. (23), the quantiles of the posterior reliability index with confidence level α, that is β_α^{up}, can be derived as follows:

$$\beta_\alpha^{up} = \exp\left[\Phi^{-1}(\alpha) \cdot \upsilon + \zeta\right] + \lambda. \tag{24}$$

Because of the posterior failure probability with α confidence level (denoted as $P_{f,\alpha}^{up}$) is a monotonous function of the posterior reliability index with 1-α confidence level (denoted as $\beta_{1-\alpha}^{up}$), the posterior failure probability with α confidence level is equal to:

$$P_{f,\alpha}^{up} = \Phi(-\beta_{1-\alpha}^{up}) = \Phi\left\{\exp\left[\Phi^{-1}(1-\alpha) \cdot \upsilon + \zeta\right] + \lambda\right\}. \tag{25}$$

From Eq. (25), it is obvious that this formula can provide the posterior failure probability at any confidence level α in an explicit form.

3.3.3. Approximation of the probability distribution of the posterior failure probability

To further derive the PDF and CDF of the posterior failure probability, it is essential to establish the relationship between the standard normal random variable U and the posterior failure probability. Similarly, the notations $f_{P_f^{up}}(P_f)$ and $F_{P_f^{up}}(P_f)$ are introduced to represent the PDF and CDF of the posterior failure probability, respectively. Based on Eq. (2) and Eq. (22), the relationship between the standard normal random variable and the posterior failure probability can be derived as:

$$U = \frac{\ln\left[-\Phi^{-1}(P_f) - \lambda\right] - \zeta}{\upsilon}. \tag{26}$$

Following this, by substituting Eq. (26) into the right-hand side of Eq. (21), the explicit CDF of the posterior failure probability can be represented as follows:

$$F_{P_f^{up}}(P_f) = \Phi\left\{\frac{-\ln\left[-\Phi^{-1}(P_f) - \lambda\right] - \zeta}{\upsilon}\right\}. \tag{27}$$

Finally, by taking the derivative on both sides of Eq. (27), the explicit PDF expression of the posterior failure probability can be readily obtained as:

$$f_{P_f^{up}}(P_f) = -\frac{\phi\left\{\frac{\ln\left[-\Phi^{-1}(P_f) - \lambda\right] - \zeta}{\upsilon}\right\}}{\upsilon \cdot \left[-\Phi^{-1}(P_f) - \lambda\right]\phi\left[\Phi^{-1}(P_f)\right]}. \tag{28}$$

Similarly as in Section 3.3.2, it is observed from Eq. (28) that the PDF of the posterior failure probability is given in the form of an explicit expression.

3.4. Procedure of the proposed method for completely characterizing the posterior failure probability

Fig. 1 outlines the steps for fully quantifying the probabilistic characteristics of the posterior failure probability, serving as a practical guide for implementing this method. The detailed steps are provided in Algorithm 1.

Algorithm 1 Complete characterization of the posterior failure probability

1. Set up the formula for calculating the posterior reliability index
   (a) define the prior distribution $f_{\boldsymbol{\Theta}}(\boldsymbol{\theta})$
   (b) define the likelihood function $L(D_{\mathbf{x}}|\boldsymbol{\theta})$
   (c) define the updating factor $\xi(\boldsymbol{\theta})$
   (d) establish the posterior reliability index formula
2. Use sparse grid numerical integration (SGNI) to generate the integration points and weights for distribution parameters $\boldsymbol{\theta}$
   (a) choose the accuracy level q and generate the set $H(q, N)$
   (b) determine the interpolation points θ_{j_h} and weights p_{j_h}
3. Evaluate the first three raw moments of the posterior reliability index $\hbar_{1B}$, $\hbar_{2B}$, and $\hbar_{3B}$ with the determined θ_{j_h} and p_{j_h} based on Eq. (9)
4. Determine the first three moments of the posterior reliability index, μ_B, σ_B, and α_{3B} according to Eqs. (12)-(14)
5. Construct the probability distribution of the posterior reliability index $f_{\beta^{up}}(\beta)$ and $F_{\beta^{up}}(\beta)$ using the shifted lognormal distribution model.
6. Obtain quantities of interest associated with the posterior failure probability
   (a) compute the mean of the posterior failure probability $\overline{P_f^{up}}$ based on Eq. (20)
   (b) evaluate the quantile of the posterior failure probability $P_{f,\alpha}^{up}$ based on Eq. (25)
   (c) obtain the PDF of the posterior failure probability $f_{P_f^{up}}(P_f)$ based on Eq. (28)
7. Check whether any additional data inspection is available.
   (a) If there is no additional data, the algorithm is terminated.
   (b) If there is additional data available:
      i) reformulate the likelihood function $L(D_{\mathbf{x}}|\boldsymbol{\theta})$
      ii) recompute the updating factor $\xi(\boldsymbol{\theta})$ under the fixed sample sets
      iii) go back to Step 3

It needs to be emphasized that in the process of evaluating step 3, once the accuracy level q of SGNI is determined, it is only necessary to perform the reliability analysis conditional on the fixed grid points during the initial update. Consequently, the outcomes of the reliability analysis obtained during the initial update can be considered in subsequent updates. It is only necessary to recalculate the updating factor $\xi(\boldsymbol{\theta})$ in Eq. (9), that changes as more data measurements are added.

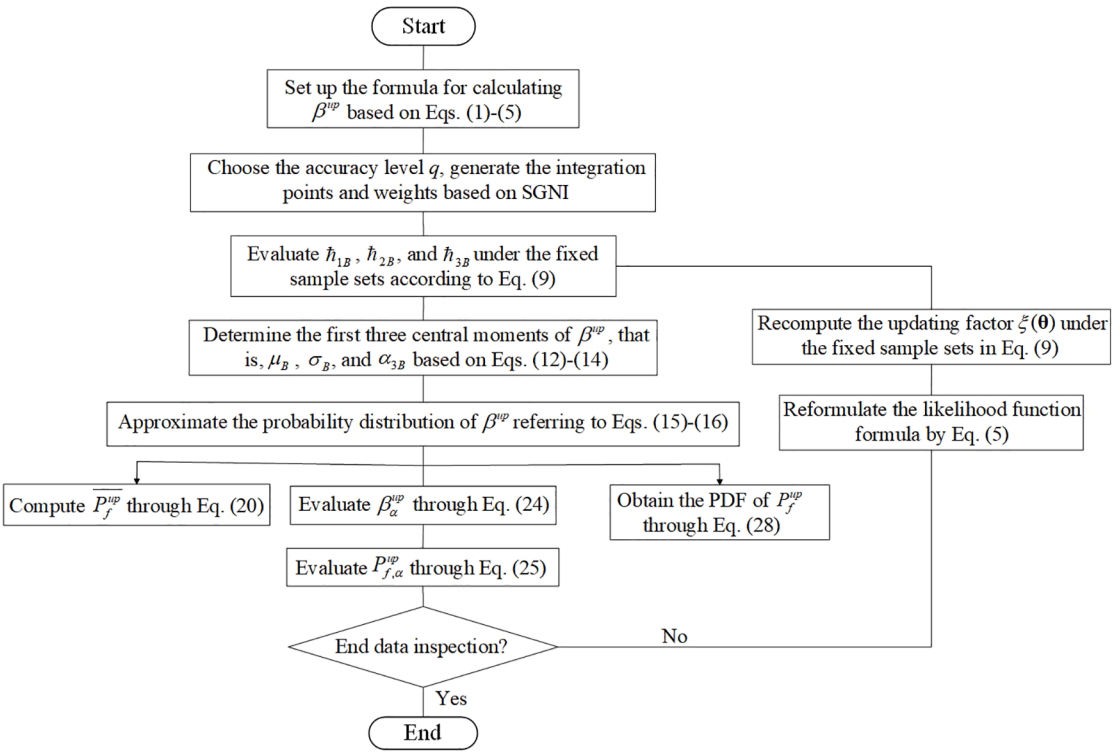

Fig. 1. Flowchart of the proposed method.

4. Numerical examples

In this section, four numerical examples are studied to validate the efficiency and precision of the proposed method. The first example considers a basic reliability analysis model to illustrate the computational procedure of the proposed method step by step. The second example investigates a corroded bending beam involving two correlated random variables. The third example deals with a two-degree-of-freedom primary–secondary system model containing multiple uncertain distribution parameters. The last example addresses a 120-bar space with an implicit limit state function. The results obtained from the proposed method were compared with those determined from the widely used simulation-based methods. More specifically, MCMC simulations [17,43] are conducted to generate samples of the distribution parameters that follow the corresponding posterior distribution. Then, for each of those samples, MCS is applied to calculate, in turn, samples of the failure probability. The latter samples are then used to construct the histograms of the posterior reliability index or the corresponding posterior failure probability.

4.1. Example 1: R-S

In the first example, the analysis focuses on a bar subjected to tension stress, a case previously studied by Zhang and Mahadevan [44]. The limit-state function can be expressed as

$$G(R,S) = R - S, \tag{29}$$

where R denotes the resistance of the bar, S denotes the corresponding applied load, and both R and S follow the normal distribution.

It is assumed that there is no uncertainty in the mean value (μ_R) and standard deviation (σ_R) of R and standard deviation (σ_s) of S, where μ_R=50 MPa, σ_R=5 MPa, σ_S=7 MPa. However, uncertainty exists in the mean value (μ_S) of S, with the prior distribution of μ_S obeying a lognormal distribution with a mean value of 35 MPa and a standard deviation of 2.0 MPa. In this case, the reliability index conditional on the distribution parameters can be expressed in a closed-form equation as

$$\beta(\boldsymbol{\theta}) = \frac{\mu_R - \mu_S}{\sqrt{\sigma_R^2 + \sigma_S^2}} = \frac{50 - \mu_S}{\sqrt{5^2 + 7^2}}. \tag{30}$$

It is assumed that 10 sets of applied load measurements are detected at $t = 10$ years and $t = 20$ years respectively, given in Fig. 2. Based on Eq. (8), the first three raw moments of the posterior reliability index at $t = 10$ years can be formulated as

$$\hbar_{lB,t=10\text{years}} = \int_{\mu_S} \left(\frac{50 - \mu_S}{\sqrt{5^2 + 7^2}} \right)^l \xi(\mu_S) f_S(\mu_S) d\mu_S \quad l = 1, 2, 3, \tag{31}$$

with the updating factor given as

$$\xi(\mu_S) = \frac{\prod_{i=1}^{10} \frac{1}{7\sqrt{2\pi}} \exp\left(-\frac{1}{2} \frac{(D_{S,i} - \mu_S)^2}{7} \right)}{\int_{\mu_S} \prod_{i=1}^{10} \frac{1}{7\sqrt{2\pi}} \exp\left(-\frac{1}{2} \frac{(D_{S,i} - \mu_S)^2}{7} \right)}. \tag{32}$$

The SGNI with the accuracy level $q = 3$ is selected for calculation, leading to 7 realizations of the applied load, as shown in Fig. 3.

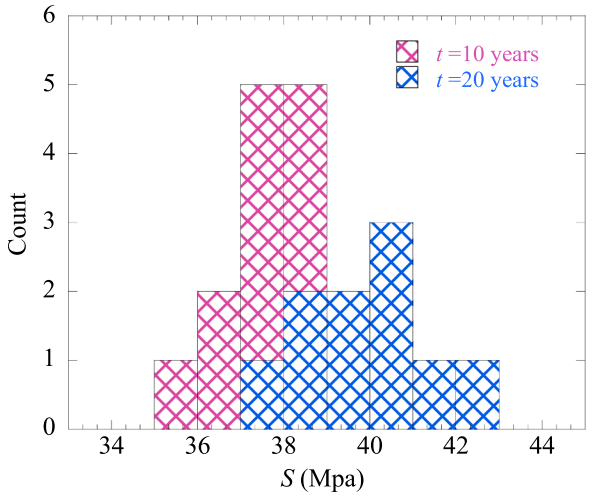

Fig. 2. Histogram of load measurement data.

Based on Eq. (9), the first three raw moments at $t = 10$ years can be estimated as $\hbar_{1B,t=10\text{years}} = 1.622$, $\hbar_{2B,t=10\text{years}} = 2.661$, and $\hbar_{3B,t=10\text{years}} = 4.416$, with the detailed calculation results listed in Table 1. Once the first three raw moments have been determined, the first three central moments of the posterior reliability index at $t = 10$ years can be calculated as $\mu_{B,t=10\text{years}} = 1.622$, $\sigma_{B,t=10\text{years}} = 0.177$, $\alpha_{3B,t=10\text{years}} = -0.044$.

In this case, the skewness $\alpha_{3B,t=10\text{years}} = -0.044$ is negative. Thus, we first adopt the absolute value of the skewness and then proceed to mirror the PDF around $\beta = 1.622$. Based on Eq. (15), the explicit PDF of the posterior reliability index at $t = 10$ years can be derived as

$$f_{\beta^{up}}(\beta) = \frac{27.331}{(13.750-\beta)} \times \exp\left\{ -2346.770[\ln(13.750-\beta) - 2.495]^2 \right\}. \tag{33}$$

Upon acquiring the explicit PDF expression of the posterior reliability index, in accordance with Eq. (20), the expected value of the posterior failure probability at $t = 10$ years can be estimated as $\overline{P_f^{up}} = 5.517 \times 10^{-2}$. In addition, after obtaining the first three moments of the posterior reliability index, any quantile of the posterior failure probability at $t = 10$ years can be given in an explicit expression according to Eq. (25), as follows:

$$P_{f,\alpha}^{up} = \Phi\left\{13.750 - \exp\left[0.0146 \cdot \Phi^{-1}(\alpha) + 2.495\right]\right\}. \tag{34}$$

According to Eq. (28), the explicit PDF expression of the posterior failure probability at $t = 10$ years is given as follows:

$$f_{P_f^{up}}(P_f) = -\frac{\phi\left(\frac{\ln\left\{-\Phi^{-1}(P_f)+13.750\right\}-2.495}{0.000426}\right)}{0.0146 \cdot \left\{-\Phi^{-1}(P_f) + 13.750\right\}\phi\left\{\Phi^{-1}(P_f)\right\}}. \tag{35}$$

Considering the data measurements collected at $t = 20$ years, only the updating factor in Eq. (32) needs to be reformulated as follows:

$$\xi(\mu_S) = \frac{\prod_{i=1}^{20} \frac{1}{7\sqrt{2\pi}} \exp\left(-\frac{1}{2}\frac{(D_{S,i}-\mu_S)^2}{7}\right)}{\int_{\mu_S} \prod_{i=1}^{20} \frac{1}{7\sqrt{2\pi}} \exp\left(-\frac{1}{2}\frac{(D_{S,i}-\mu_S)^2}{7}\right)}. \tag{36}$$

Based on Eqs. (9)-(14), the first three central moments of the posterior reliability index are obtained as $\mu_{B,t=20\text{years}} = 1.478$, $\sigma_{B,t=20\text{years}} = 0.140$, and $\alpha_{3B,t=20\text{years}} = -0.172$ respectively, with the detailed calculation results for obtaining its first three raw moments are also presented in Table 1. Table 1 reveals that the values of the grid points of SGNI, the first three moments of the posterior reliability index, and their associated weights have been determined and remain unchanged since the initial update. The only calculation required in the subsequent update is the updating factor, determined by estimating the newly formulated likelihood function under the fixed grid points of SGNI. Having acquired the first three central moments of the posterior reliability index, the above steps can be readily employed to derive the PDF of the posterior reliability index, compute the mean value of the posterior failure probability, estimate the quantiles of the posterior failure probability, and determine the PDF of the posterior failure probability.

Fig. 4 shows the comparison between the histograms generated via MCMC combined with MCS (100,000 samples) and the proposed method with respect to the posterior reliability index for the first ($t = 10$ years) and second ($t = 20$ years) update. As can be seen

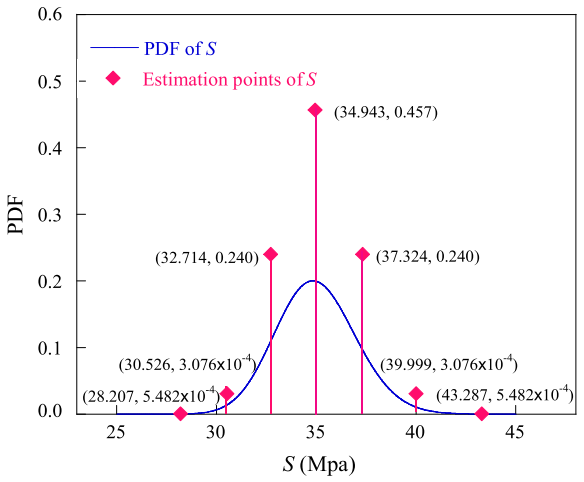

Fig. 3. Estimation points and weights of the applied load.

Table 1
Detailed calculations for the first three raw moments of the posterior reliability index.

Years	S	p_{jh}	$\beta(\cdot)$	$\beta^2(\cdot)$	$\beta^3(\cdot)$	$\xi(\cdot)$	
$t=10$	$\begin{Bmatrix}28.207\\30.526\\32.714\\34.943\\37.324\\39.999\\43.287\end{Bmatrix}$	$\begin{Bmatrix}5.482\times10^{-4}\\3.076\times10^{-2}\\0.240\\0.457\\0.240\\3.076\times10^{-2}\\5.482\times10^{-4}\end{Bmatrix}$	$\begin{Bmatrix}2.533\\2.264\\2.009\\1.750\\1.474\\1.163\\0.780\end{Bmatrix}$	$\begin{Bmatrix}6.418\\5.125\\4.038\\3.064\\2.171\\1.352\\0.609\end{Bmatrix}$	$\begin{Bmatrix}16.258\\11.601\\8.114\\5.363\\3.200\\1.571\\0.475\end{Bmatrix}$	$\begin{Bmatrix}3.404\times10^{-5}\\1.505\times10^{-3}\\1.965\times10^{-2}\\9.860\times10^{-2}\\1.802\times10^{-1}\\8.923\times10^{-2}\\5.086\times10^{-3}\end{Bmatrix}$	$\hbar_{1B}=1.622$ $\hbar_{2B}=2.661$ $\hbar_{3B}=4.416$
$t=20$	Same	Same	Same	Same	Same	$\begin{Bmatrix}5.108\times10^{-11}\\3.400\times10^{-7}\\1.840\times10^{-4}\\1.502\times10^{-2}\\1.763\times10^{-1}\\1.775\times10^{-1}\\3.274\times10^{-3}\end{Bmatrix}$	$\hbar_{1B}=1.478$ $\hbar_{2B}=2.203$ $\hbar_{3B}=3.313$

from Fig. 4 that the histogram of posterior reliability index obtained from MCMC combined with MCS possesses a shape which can be appropriately captured by the proposed approach. In addition, the PDF curves of the posterior reliability index obtained from the proposed method fit well with these histograms, which only requires 7 reliability index evaluations conditional on the fixed estimate points at the first update and does not require additional reliability index evaluations as well as the posterior samples acquisition in the subsequent update.

Fig. 5 shows the comparison between the histograms of the posterior failure probability and the curves obtained from the proposed method. It can be seen from Fig. 5 that the histograms of posterior failure probability tilt more to the left, and the curves derived from the proposed method can agree well with the histograms of posterior failure probability.

Table 2 compares the expected value of the posterior failure probability, the quantiles of the posterior failure probability as well as the computation efficiency between the MCMC combined with MCS (MCMC+MCS) (100,000 samples) with the proposed method. It can be observed from Table 2 that: 1) the expected value and the quantiles of the posterior failure probability are nearly the same as the results determined from MCMC combined with MCS; 2) the proposed method can obtain the expected value and the quantiles of the posterior failure probability with only 7 evaluations of the reliability index at the first update time ($t=10$ years), with no additional reliability analysis and posterior samples acquisition for subsequent updates.

4.2. *Example 2: Corroded bending beam*

The second example investigates a corroded bending beam as depicted in Fig. 6, which was modified from Ping et al. [45]. This beam is submitted to dead load and a concentrated load F applied at midspan, and the structural failure is defined as maximal normal stress exceeding the allowable stress $[\sigma]$. The limit state function of this beam can be expressed as

$$G(\mathbf{X}) = [\sigma] - \sigma_{\max}, \tag{37}$$

where $[\sigma]=500$Mpa denotes the allowable stress and $\sigma_{\max}$ denotes the maximal normal stress that can be given as

$$\sigma_{\max} = M/W, \tag{38}$$

where $W{=}bh^2/6$ denotes the bending section coefficient and M denotes the maximal bending moments

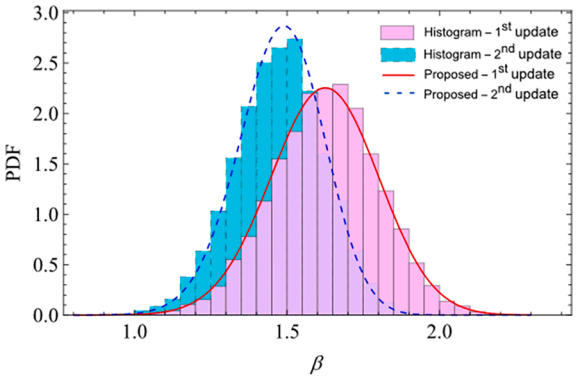

Fig. 4. Histogram and PDF of the posterior reliability index.

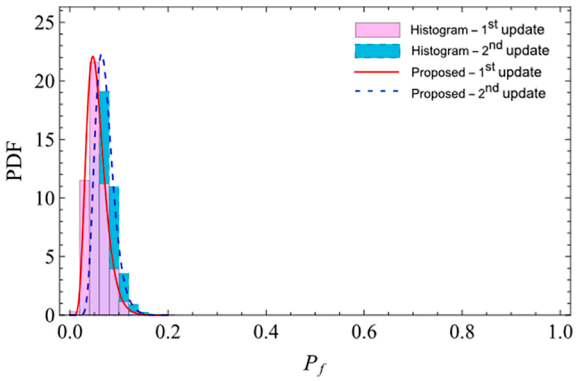

Fig. 5. Histogram and PDF of the posterior failure probability.

Table 2
Results comparison between the proposed method and MCMC+MCS of Example 1.

	Method	NoRE[a]	$\overline{P_f^{up}}$	$P_{f,0.75}^{up}$	$P_{f,0.9}^{up}$
1st update	MCMC+MCS	100,000	5.453×10^{-2}	6.526×10^{-2}	8.060×10^{-2}
	Proposed	7	5.517×10^{-2} (1.17 %)	6.643×10^{-2} (1.79 %)	8.168×10^{-2} (1.34 %)
2nd update	MCMC+MCS	100,000	7.224×10^{-2}	8.420×10^{-2}	9.924×10^{-2}
	Proposed	0	7.168×10^{-2} (−0.78 %)	8.289×10^{-2} (−1.56 %)	9.741×10^{-2} (−1.84 %)

Note: [a]Number of reliability index evaluations (NoRE); Values in parentheses are the relative errors of the proposed method compared to MCMC+MCS.

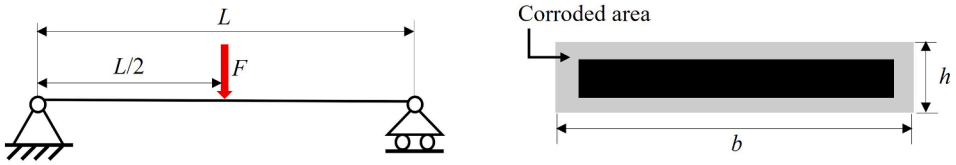

(a) Corroded bending beam (b) Residual area

Fig. 6. Corroded bending beam under a midspan load for Example 2.

$$M = \frac{FL}{4} + \frac{\rho_{st} bhL^2}{8}, \tag{39}$$

where L denotes the length of the beam, ρ_{st} denotes the steel mass density of the beam, b denotes the beam section width, and h denotes the beam section height.

For this example, assume that the correlation coefficient between beam section height h and beam section width b is 0.4, and that there is uncertainty in the mean and standard deviation of both b and h. Table 3 provides the statistical information concerning these random variables and the prior information for these distribution parameters.

Table 3
Statistical information of the random variables for Example 2.

Variables	Distribution	Mean	Standard deviation	Correlation coefficient
b (m)	Normal	N (0.2, 0.03)	LN ($0.03, 4.5 \times 10^{-3}$)	$\begin{pmatrix} 1 & 0.4 & 0 & 0 \\ 0.4 & 1 & 0 & 0 \\ 0 & 0 & 0 & 0 \\ 0 & 0 & 0 & 0 \end{pmatrix}$
h (m)	Normal	N ($0.03, 4.5 \times 10^{-3}$)	LN ($4.5 \times 10^{-3}, 6.75 \times 10^{-4}$)	
F (N)	Lognormal	3500	700	
L (m)	Lognormal	5	0.5	
ρ_{st} (kN·m^3)	Deterministic	78.5	–	

Note: N (μ, σ) represents a normal random variable with a mean of μ and a standard deviation of σ; LN (μ, σ) represents a lognormal random variable with a mean of μ and a standard deviation σ.

The steel beam's cross-section is isotropic and experience exponential degeneration over time [46]. It is assumed that two sets of data measurements for b and h are collected sequentially at different times, given as $D_{\mathbf{X},1} = \{D_{b,1} = 0.18, D_{h,1} = 0.026\}$ and $D_{\mathbf{X},2} = \{D_{b,2} = 0.14, D_{h,2} = 0.019\}$. In this case, the likelihood function can be formulated as $L(D_{\mathbf{X}}|\boldsymbol{\theta}) = \prod_{i=1}^{N_d} \frac{1}{\sqrt{(2\pi)^{N_d}|\boldsymbol{\Sigma}_{\boldsymbol{\theta}}|}} \exp\left(-\frac{1}{2}\left(D_{\mathbf{X},i} - \boldsymbol{\mu}_{\boldsymbol{\theta}}\right)^T \boldsymbol{\Sigma}_{\boldsymbol{\theta}}^{-1} \left(D_{\mathbf{X},i} - \boldsymbol{\mu}_{\boldsymbol{\theta}}\right)^T \right)$, where the hyper mean $\boldsymbol{\mu}_{\boldsymbol{\theta}} = (\mu_b, \mu_h)^{\mathrm{T}}$ and the hyper covariance $\boldsymbol{\Sigma}_{\boldsymbol{\theta}} = \begin{pmatrix} \sigma_b^2 & 0.4\sigma_b\sigma_h \\ 0.4\sigma_b\sigma_h & \sigma_h^2 \end{pmatrix}$.

Since there is a correlation coefficient between b and h, in this example, the orthogonal normal transformation [47] is used to evaluate the reliability index conditional on the fixed estimate points determined by SGNI. Due to the complexity and larger variability of the likelihood function, SGNI with an accuracy level $q = 5$ was selected here, and a total of 2001 sets of fixed estimate points for four distribution parameters were generated. Based on Eqs. (9)-(14) combined with the orthogonal normal transformation, when considering the first set of inspections ($N_d = 1$), the first three central moments of the posterior reliability index can be determined as $\mu_{B,\text{update1}} = 1.667$, $\sigma_{B,\text{update1}} = 0.576$, and $\alpha_{3B,\text{update1}} = 0.225$. While considering the second set of inspections ($N_d = 2$), the first three central moments of the posterior reliability index can be obtained as $\mu_{B,\text{update2}} = 1.078$, $\sigma_{B,\text{update2}} = 0.460$, and $\alpha_{3B,\text{update2}} = -0.018$. According to the proposed method, the probabilistic characteristics of the posterior failure probability can be fully characterized with the help of the obtained first three central moments of the posterior reliability index.

Fig. 7 shows the comparison between the histograms generated using a combination of MCMC and MCS (100,000 samples) and the curves obtained from the proposed method. In Fig. 7, it is obvious that the histograms of the posterior reliability index exhibit a bell-shaped distribution that is easy to fit. The red line for the first update and the blue spot line for the second update of the posterior reliability index obtained from the proposed method fit well with the histograms of posterior reliability index generated by the MCMC combined with MCS.

In Fig. 8, a comparison is made between the histograms of the posterior failure probability and the curves generated by the proposed method. As shown in Fig. 8, the histograms of the posterior failure probability are tilted to the left and have large variability, which is not easy to fit. However, the curves derived from the proposed method fit almost perfectly with the histograms of the posterior failure probability.

Table 4 provides a comparative analysis between the MCMCS+MCS and the proposed method, including the mean and quantiles of the posterior failure probability and their computation efficiency. It can be found from Table 4 that: 1) the outcomes determined through the proposed method for the mean and the quantiles of the posterior failure probability are close to the results obtained from the combination of MCMC and MCS. This illustrates that the proposed method has good applicability to update the cases where the random variables are correlated; 2) the proposed method requires 2001 evaluations of the reliability index during the initial update time to obtain the mean and any desired quantile of the posterior failure probability due to the complexity and large variability of the likelihood function. However, for the subsequent update, the proposed method can determine these interested values without the need to perform additional computationally expensive reliability analyzes or reacquire the posterior samples of the distribution parameters.

4.3. Example 3: Two degree-of-freedom system

In the third example, a two degree-of-freedom primary–secondary oscillator subjected to a white noise base acceleration is explored, as depicted in Fig. 9. This example has been adapted from the work of Der Kiureghian and De Stefano [48]. The failure of the system is characterized by the surpassing of the peak response of the secondary spring during the duration of the excitation. The expression for the limit state function is as follows:

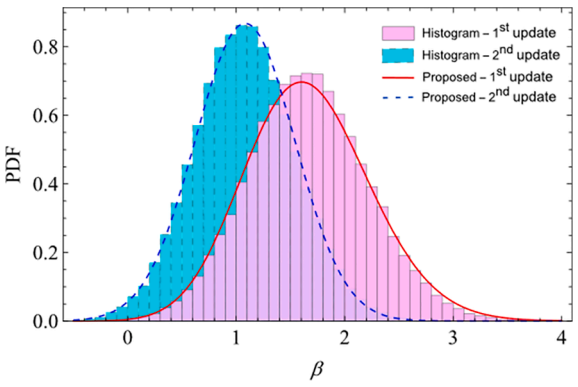

Fig. 7. Histogram and PDF of the posterior reliability index.

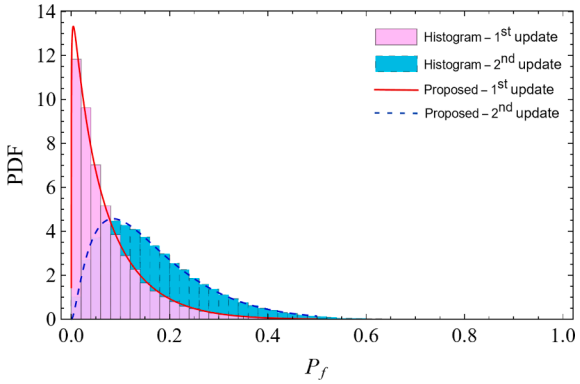

Fig. 8. Histogram and PDF of the posterior failure probability.

Table 4
Results comparison between the proposed method and MCMC+MCS of Example 2.

	Method	NoRE[a]	$\overline{P_f^{ip}}$	$P_{f,0.75}^{ip}$	$P_{f,0.9}^{ip}$
1st update	MCMC+MCS	100,000	7.296×10^{-2}	9.999×10^{-2}	1.702×10^{-1}
	Proposed	2001	7.363×10^{-2} (0.92 %)	9.836×10^{-2} (−1.63 %)	1.798×10^{-1} (5.64 %)
2nd update	MCMC+MCS	100,000	1.636×10^{-1}	2.209×10^{-1}	3.126×10^{-1}
	Proposed	0	1.634×10^{-1} (−0.12 %)	2.221×10^{-1} (0.54 %)	3.119×10^{-1} (−0.22 %)

Note: [a]Number of reliability index evaluations (NoRE); Values in parentheses are the relative errors of the proposed method compared to MCMC+MCS.

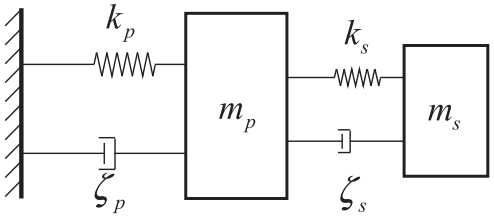

Fig. 9. Two degree-of-freedom system for Example 3.

Table 5
Statistical information of the random variables for Example 3.

Variables	Distribution	Mean	Standard deviation
m_p	Normal	N (1.0, 0.1)	LN (0.15, 7.5×10^{-3})
m_s	Normal	N (0.05, 0.005)	LN (7.5×10^{-3}, 3.75×10^{-4})
F_s	Lognormal	10	0.1
S_0	Lognormal	100.0	10
k_p	Normal	N (1.0, 0.1)	LN (0.15, 7.5×10^{-3})
k_s	Normal	N (0.01, 0.001)	LN (1.5×10^{-3}, 7.5×10^{-5})
ζ_p	Lognormal	5×10^{-2}	1×10^{-2}
ζ_s	Lognormal	2×10^{-2}	5×10^{-3}

Note: N (μ, σ) represents a normal random variable with a mean of μ and a standard deviation of σ; LN (μ, σ) represents a lognormal random variable with a mean of μ and a standard deviation σ.

$$G(\mathbf{X}) = F_s - 3k_s\sqrt{\frac{\pi S_0}{4\zeta_s\omega_s^3}\left[\frac{\zeta_a\zeta_s}{\zeta_p\zeta_s\left(4\zeta_a^2+\theta^2\right)+\gamma\zeta_a^2}\frac{\left(\zeta_p\omega_p^3+\zeta_s\omega_s^3\right)\omega_p}{\zeta_a\omega_a^4}\right]}, \tag{40}$$

where F_s represents the force capacity of the secondary spring, S_0 represents the intensity of white noise, k_s and k_p represent the spring stiffnesses, m_p and m_s represent the masses, ζ_p and ζ_s represent the damping rates natural frequencies, $\omega_p = (k_p/m_p)^{1/2}$, $\omega_s = (k_s/m_s)^{1/2}$, $\omega_a = (\omega_p + \omega_s)/2$, $\theta = (\omega_p - \omega_s)/\omega_a$, $\gamma = m_s/m_p$, and $\zeta_a = (\zeta_p + \zeta_s)/2$; and the subscripts p refer to the primary oscillators and subscripts s refer to the secondary oscillators.

Due to the imperfect state knowledge of the structural parameters m_p, m_s, k_p, and k_s, the mean and standard deviation of these structural parameters are assumed uncertain. Table 5 gives the statistical information of random variables involved in this example as well as the prior information for these distribution parameters.

In this example, two sets of inspections for structural parameters m_p, m_s, k_p, k_s are collected sequentially, given as $D_{\mathbf{X},1}$={$D_{m_p,1} = 1.2$, $D_{m_s,1} = 0.06$, $D_{k_p,1} = 0.9$, $D_{k_s,1} = 0.012$} and $D_{\mathbf{X},2}$={$D_{m_p,2} = 1.0$, $D_{m_s,2} = 0.04$, $D_{k_p,2} = 1.1$, $D_{k_s,2} = 0.01$}. The likelihood function can be formulated as $L(D_{\mathbf{X}}|\boldsymbol{\theta}) = \prod_{i=1}^{N_d}\frac{1}{\sqrt{(2\pi)^{N_d}|\boldsymbol{\Sigma}_{\boldsymbol{\theta}}|}}\exp\left(-\frac{1}{2}\left(D_{\mathbf{X},i}-\boldsymbol{\mu}_{\boldsymbol{\theta}}\right)^T\boldsymbol{\Sigma}_{\boldsymbol{\theta}}^{-1}\left(D_{\mathbf{X},i}-\boldsymbol{\mu}_{\boldsymbol{\theta}}\right)^T\right)$, where the hyper mean $\boldsymbol{\mu}_{\boldsymbol{\theta}} = \left(\mu_{m_p}, \mu_{m_s}, \mu_{k_p}, \mu_{k_s}\right)^T$ and the hyper covariance $\boldsymbol{\Sigma}_{\boldsymbol{\theta}} = \mathrm{diag}\left(\sigma_{m_p}^2, \sigma_{m_s}^2, \sigma_{k_p}^2, \sigma_{k_s}^2\right)$. Execute the computation procedure of the proposed method as mentioned above, since this example involves eight uncertain distribution parameters, a total of 1105 fixed sample sets were generated through the SGNI ($q = 3$).

The PDF curves of the posterior reliability index obtained from the proposed method are shown in Fig. 10, compared with the histograms (100,000 samples) generated using MCMC combined with MCS. Likewise, the histograms of the posterior reliability index exhibit a favorable shape (bell-shaped) distribution that is not difficult to fit, and the curves of the posterior reliability index obtained from the proposed method can fit the histograms well.

Then, Fig. 11 presents the PDF curves of the posterior failure probability derived from the proposed method, compared with the histograms (100,000 samples) of the posterior failure probability determined by MCMC combined with MCS. Fig. 11 clearly indicates that the histograms of the posterior failure probability are heavily skewed to the left, but the curves derived from the proposed method can still agree well with the histograms of the posterior failure probability.

The calculation results and efficiency of the proposed method are presented in Table 6, as well as the results obtained by the combination of MCMC and MCS (100,000 samples). It is indicated in Table 6 that: 1) the results of the mean and quantile of the posterior failure probability are almost the same as those obtained by MCS combined with MCMCS. Consequently, the proposed method exhibits applicability to problems involving multi-dimensional distribution parameter updates; 2) the proposed method requires only 1105 times of reliability index evaluations within the first update time to obtain the mean and any quantiles of the posterior failure probability. In the subsequent update process, there is no need to perform any additional reliability analysis and acquisition of posterior samples.

4.4. Example 4: 120-bar space truss structure

The last example considers a 120-bar space truss structure as illustrated in Fig. 12, which has been investigated by Dang et al. [49]. This structure is a three-dimensional finite element model comprising 49 nodes and 120 elements. Nodes 0, 1, 4, 7 and 10 are subjected to concentrated loads along the negative z-axial, given as P_0, P_1, P_4, P_7, and P_{10} respectively. The limit-state function of this structure can be defined as

$$G(\mathbf{X}) = \Delta - V(E, A, P_0, P_1, P_4, P_7, P_{10}), \tag{41}$$

where $\Delta = 55$ mm denotes a vertical threshold, E denotes the Young's modulus of the material, A denotes the cross-sectional area, $V(\cdot)$ denotes the vertical displacement of the top nodes, which can be analyzed by the finite-element software, OpenSees.

In this example, the mean values of P_0, P_1, P_4, P_7, and P_{10} are considered to be uncertain. The statistical information for random variables involved in this example and the prior information for the distribution parameters μ_{P_0}, μ_{P_1}, μ_{P_4}, μ_{P_7}, and $\mu_{P_{10}}$ are given in Table 7.

Assume that two sets of data measurements for the vertical point load P_0, P_1, P_4, P_7, and P_{10} are collected sequentially at different times, given as $D_{\mathbf{X},1}$={$D_{P0,1} = 495$, $D_{P1,1} = 153$, $D_{P4,1} = 176$, $D_{P7,1} = 165$, $D_{P10,1} = 198$} and $D_{\mathbf{X},2}$={$D_{P0,2} = 512$, $D_{P1,2} = 168$, $D_{P4,2} = 145$, $D_{P7,2} = 135$, $D_{P10,2} = 171$}. The likelihood function is $L(D_{\mathbf{X}}|\boldsymbol{\theta}) = \prod_{i=1}^{N_d}\frac{1}{\sqrt{(2\pi)^{N_d}|\boldsymbol{\Sigma}|}}\exp\left(-\frac{1}{2}\left(D_{\mathbf{X},i}-\boldsymbol{\mu}_{\boldsymbol{\theta}}\right)^T\boldsymbol{\Sigma}^{-1}\left(D_{\mathbf{X},i}-\boldsymbol{\mu}_{\boldsymbol{\theta}}\right)^T\right)$, where the hyper mean $\boldsymbol{\mu}_{\boldsymbol{\theta}} = \left(\mu_{P_0}, \mu_{P_1}, \mu_{P_4}, \mu_{P_7}, \mu_{P_{10}}\right)^T$ and $\boldsymbol{\Sigma} = \mathrm{diag}(100^2, 40^2, 40^2, 40^2, 40^2)$.

By performing the calculation procedure of the proposed method as illustrated in Examples 1–3, one can easily obtain the PDF of the posterior reliability index, the mean, the quantile, and even the PDF of the posterior failure probability. In this process, based on SGNI ($q = 3$), a total of 341 sets of fixed estimate points for five distribution parameters were generated.

Fig. 13 presents the PDF curves derived from the proposed method compared with the histograms (100,000 samples) generated using MCMCS combined with MCS. This figure is given to compare the fit of the curves obtained from the proposed method to the histograms for both first and second updates of the posterior reliability index. As shown in Fig. 13, it is evident that the histogram of the posterior reliability index has a desirable shape (bell-shaped distribution), and the curves produced by the proposed method fit it quite

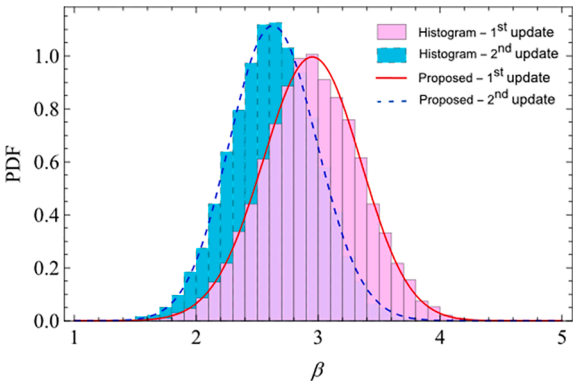

Fig. 10. Histogram and PDF of the posterior reliability index.

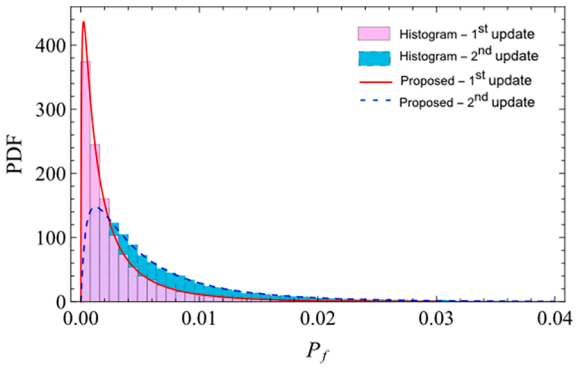

Fig. 11. Histogram and PDF of the posterior failure probability.

Table 6
Results comparison between the proposed method and MCMC+MCS of Example 3.

	Method	NoRE[a]	$\overline{P_f^{up}}$	$P_{f,0.75}^{up}$	$P_{f,0.9}^{up}$
1st update	MCMC+MCS	100,000	3.176×10^{-3}	3.711×10^{-3}	7.612×10^{-3}
	Proposed	1105	3.188×10^{-3} (0.38 %)	3.797×10^{-3} (2.32 %)	7.547×10^{-3} (−0.85 %)
2nd update	MCMC+MCS	100,000	6.501×10^{-3}	8.260×10^{-3}	1.450×10^{-2}
	Proposed	0	6.472×10^{-3} (−1.14 %)	8.332×10^{-3} (0.87 %)	1.459×10^{-2} (0.62 %)

Note: [a]Number of reliability index evaluations (NoRE); Values in parentheses are the relative errors of the proposed method compared to MCMC+MCS.

well.

In addition, the PDF curves of the posterior failure probability derived from the proposed method are given in Fig. 14, together with the histograms of the posterior failure probability determined from the combination of MCMC and MCS (100,000 samples). As depicted in Fig. 14, the samples of the histograms are mainly concentrated in the range of the posterior failure probability of 0–0.1, which shows a small variability. The PDF curves of the posterior failure probability derived from the proposed method can still agree well with the histograms of the posterior failure probability in this situation.

To further show the mean and quantile of the posterior failure probability of the proposed method and its efficiency, the outcomes determined from the proposed method were compared with those obtained from the MCMC combined with MCS (100,000 samples) in Table 8. The data in Table 8 indicates that: 1) the mean and quantiles of the posterior failure probability achieved using the proposed method closely match those obtained through MCMC combined with MCS. Therefore, the proposed method is well-suited for addressing problems involving implicit performance function; 2) the proposed method requires only 341 evaluations of the reliability index during the first update to obtain the mean and any quantiles of the posterior failure probability without any additional reliability analysis and posterior sample acquisition in the subsequent updates.

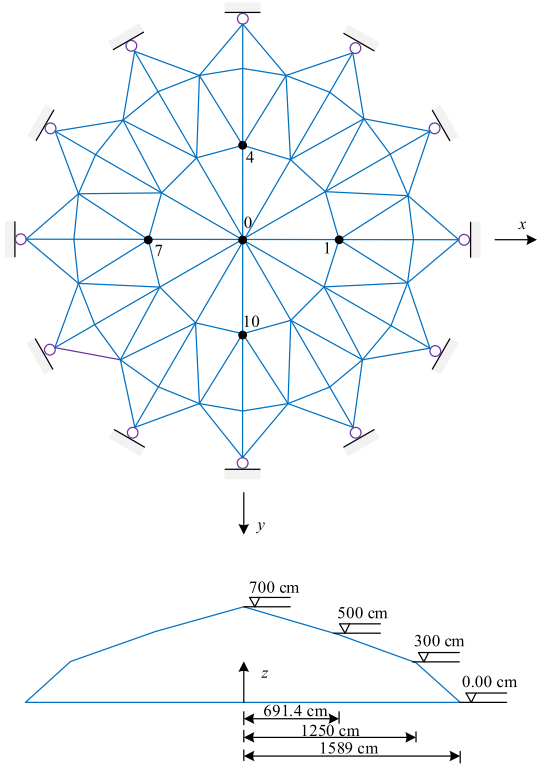

Fig. 12. A 120-bar space truss structure for Example 4.

Table 7
Statistical information of the random variables for Example 4.

Variables	Distribution	Mean	Standard deviation
E (MPa)	Lognormal	200,000	30,000
A (mm^2)	Lognormal	2000	200
P_0 (kN)	Normal	N (500, 50)	100
P_1 (kN)	Normal	N (200, 20)	40
P_4 (kN)	Normal	N (200, 20)	40
P_7 (kN)	Normal	N (200, 20)	40
P_{10} (kN)	Normal	N (200, 20)	40

Note: N (μ, σ) represents a normal random variable with a mean of μ and a standard deviation of σ; LN (μ, σ) represents a lognormal random variable with a mean of μ and a standard deviation σ.

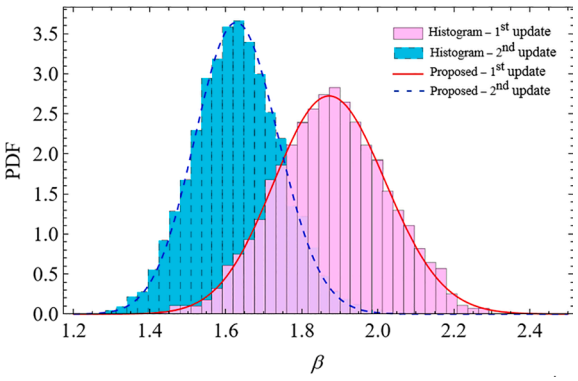

Fig. 13. Histogram and PDF of the posterior reliability index.

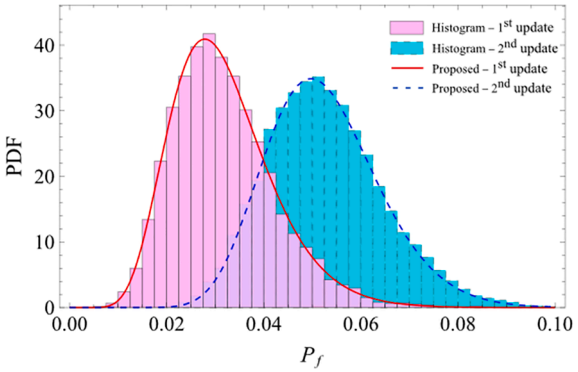

Fig. 14. Histogram and PDF of the posterior failure probability.

Table 8
Results comparison between the proposed method and MCMC+MCS of Example 4.

	Method	NoRE[a]	$\overline{P_f^{up}}$	$P_{f,0.75}^{up}$	$P_{f,0.9}^{up}$
1st update	MCMC+MCS	100,000	3.174×10^{-2}	3.779×10^{-2}	4.587×10^{-2}
	Proposed	341	3.171×10^{-2} (−0.09 %)	3.770×10^{-2} (−0.24 %)	4.576×10^{-2} (−0.24 %)
2nd update	MCMC+MCS	100,000	5.266×10^{-2}	6.032×10^{-2}	6.905×10^{-2}
	Proposed	0	5.249×10^{-2} (−0.32 %)	5.968×10^{-2} (1.06 %)	6.815×10^{-2} (−1.30 %)

Note: [a]Number of reliability index evaluations (NoRE); Values in parentheses are the relative errors of the proposed method compared to MCMC+MCS.

5. Conclusions

This paper presents an efficient framework designed to comprehensively characterize the probabilistic properties of the posterior failure probability. In the proposed method, the sparse grid numerical integration is recommended to evaluate the first three moments of the posterior reliability index, allowing for the reuse of results obtained from initial analyses. Then, the shifted lognormal distribution is employed to approximate the probability distribution of the posterior reliability index. Finally, utilizing the distribution information of the posterior reliability index enables the straightforward determination of the mean, quantiles, and the probability distribution of the posterior failure probability. Four numerical examples were studied, and the conclusions can be drawn as follows:

- To estimate the quantity of interest for the posterior failure probability, the proposed method can re-utilize the outcomes of the reliability index evaluations conditional on the determined distribution parameter sample sets obtained in the initial update. Therefore, when multiple updates are required, no additional reliability analyses are required.
- The proposed method can separate the effect of aleatory and epistemic uncertainty on the posterior failure probability and provide analytical solutions for the quantiles and probability distribution of the posterior failure probability with the help of the probability distribution of the posterior reliability index.
- Four numerical examples were investigated: failure probability with explicit expression, correlated random variables, multi-dimensional distribution parameters, as well as implicit limit-state function. The findings revealed that the results obtained through the proposed method were generally in agreement with those obtained through MCMC combined with MCS, which shows that the results of the proposed method are sufficiently accurate.

In the current framework, the sparse grid numerical integration and the shifted lognormal distribution were suggested as tools to evaluate the first three moments of the posterior reliability index and approximate its probability distribution. Therefore, the proposed method inherits their limitations. That is, the efficiency of the proposed framework will be affected when dealing with a large amount of data measurements, more complex likelihood functions, high-dimensional distribution parameters, and significant epistemic uncertainty. Additionally, if the posterior reliability index is multimodal, the proposed method can no longer be used. These shortcomings can be solved by replacing the corresponding tools with some more efficient ones. Further research will be conducted to address large data measurements, complex likelihood functions, high-dimensional distribution parameters, significant epistemic uncertainty, and cases where the posterior reliability index is multimodal. In particular, future efforts will aim at approximating the probability of failure (or the reliability index) using a Gaussian process. In that way, costly evaluations of the failure probability can be replaced by the estimates provided by the Gaussian process. Furthermore, it is possible to control the error in the estimation and to

perform active learning to improve the quality of this surrogate. Another path for future developments consists of characterizing the posterior failure probability considering information beyond the first three moments employed in this work. A possibility is considering fractional moments, which carry information about all integer moments.

CRediT authorship contribution statement

Pei-Pei Li: Writing – review & editing, Writing – original draft, Validation, Software, Methodology, Investigation, Funding acquisition, Conceptualization. **Yan-Gang Zhao:** Writing – review & editing, Methodology, Funding acquisition, Conceptualization. **Chao Dang:** Writing – review & editing, Software. **Matteo Broggi:** Writing – review & editing, Methodology. **Marcos A. Valdebenito:** Writing – review & editing, Methodology, Conceptualization. **Matthias G.R. Faes:** Writing – review & editing, Supervision, Methodology, Funding acquisition, Conceptualization.

Declaration of competing interest

The authors declare that they have no known competing financial interests or personal relationships that could have appeared to influence the work reported in this paper.

Data availability

Data will be made available on request.

Acknowledgment

The authors gratefully acknowledge the support of the Alexander von Humboldt Foundation for the postdoctoral grant of Pei-Pei Li, the Henriette Herz Scouting program (Matthias G.R. Faes), and the National Natural Science Foundation of China (Grant No.: 51738001).

References

[1] M. Faes, M. Imholz, D. Vandepitte, D. Moens, A review of interval field approaches for uncertainty quantification in numerical models, Modern Trends in Structural and Solid Mechanics 3: Non-deterministic Mechanics, 2021, pp. 95-110.
[2] A. Abdollahi, H. Shahraki, M. Faes, M. Rashki, Soft Monte Carlo Simulation for imprecise probability estimation: A dimension reduction-based approach, Struct. Saf. 106 (2024) 102391.
[3] M.A. Valdebenito, M. Beer, H.A. Jensen, J.B. Chen, P.F. Wei, Fuzzy failure probability estimation applying intervening variables, Struct. Saf. 83 (2020) 101909.
[4] A. Der Kiureghian, Measures of structural safety under imperfect states of knowledge, J. Struct. Eng. 115 (1989) 1119–1140.
[5] A. Der Kiureghian, O. Ditlevsen, Aleatory or epistemic? Does it matter? Struct. Saf. 31 (2009) 105–112.
[6] M. Faes, M. Daub, S. Marelli, E. Patelli, M. Beer, Engineering analysis with probability boxes: A review on computational methods, Struct. Saf. 93 (2021) 102092.
[7] M.A. Valdebenito, X.K. Yuan, M. Faes, Augmented first-order reliability method for estimating fuzzy failure probabilities, Struct. Saf. 105 (2023) 102380.
[8] A.H.S. Ang, W.H. Tang, Probability concepts in engineering: emphasis on applications in civil and environmental engineering, John Wiley & Sons, 2007.
[9] J.B. Chen, Z.Q. Wan, A compatible probabilistic framework for quantification of simultaneous aleatory and epistemic uncertainty of basic parameters of structures by synthesizing the change of measure and change of random variables, Struct. Saf. 78 (2019) 76–87.
[10] Y.G. Zhao, P.P. Li, Z.H. Lu, Efficient evaluation of structural reliability under imperfect knowledge about probability distributions, Reliab. Eng. Syst. Saf. 175 (2018) 160–170.
[11] P.P. Li, Z.H. Lu, Y.G. Zhao, An effective and efficient method for structural reliability considering the distributional parametric uncertainty, Appl. Math. Model. 106 (2022) 507–523.
[12] C.J. Roy, W.L. Oberkampf, A comprehensive framework for verification, validation, and uncertainty quantification in scientific computing, Comput. Methods Appl. Mech. Eng. 200 (2011) 2131–2144.
[13] T. Yang, D. Xie, Z. Li, H. Zhu, Recent advances in wearable tactile sensors: Materials, sensing mechanisms, and device performance, Mater. Sci. Eng.: R: Rep. 115 (2017) 1–37.
[14] G.E. Box, G.C. Tiao, Bayesian inference in statistical analysis, John Wiley & Sons, 2011.
[15] O. Sedehi, C. Papadimitriou, L.S. Katafygiotis, Hierarchical Bayesian uncertainty quantification of Finite Element models using modal statistical information, Mech. Syst. Signal Process. 179 (2022) 109296.
[16] J.L. Beck, S.K. Au, M.W. Vanik, Monitoring structural health using a probabilistic measure, Comput. Aided Civ. Infrastruct. Eng. 16 (2001) 1–11.
[17] J.L. Beck, S.K. Au, Bayesian updating of structural models and reliability using Markov chain Monte Carlo simulation, J. Eng. Mech. 128 (2002) 380–391.
[18] J.Q. Wang, Z.Z. Lu, L. Wang, K.X. Feng, New perspective on reliability updating with equality information under line sampling, Struct. Saf. 103 (2023) 102347.
[19] Z. Wang, A. Shafieezadeh, Highly efficient Bayesian updating using metamodels: An adaptive Kriging-based approach, Struct. Saf. 84 (2020) 101915.
[20] C. Dang, P. Wei, M.G. Faes, M.A. Valdebenito, M. Beer, Parallel adaptive Bayesian quadrature for rare event estimation, Reliab. Eng. Syst. Saf. 225 (2022) 108621.
[21] C. Zhang, Z. Wang, A. Shafieezadeh, Error quantification and control for adaptive kriging-based reliability updating with equality information, Reliab. Eng. Syst. Saf. 207 (2021) 107323.
[22] H. Li, C.-G. Huang, C.G. Soares, A real-time inspection and opportunistic maintenance strategies for floating offshore wind turbines, Ocean Eng. 256 (2022) 111433.
[23] G. Walter, S.D. Flapper, Condition-based maintenance for complex systems based on current component status and Bayesian updating of component reliability, Reliab. Eng. Syst. Saf. 168 (2017) 227–239.
[24] W.H. Zhang, J.J. Qin, D.G. Lu, M. Liu, M.H. Faber, Quantification of the value of condition monitoring system with time-varying monitoring performance in the context of risk-based inspection, Reliab. Eng. Syst. Saf. 108993 (2022).
[25] C. Papadimitriou, J.L. Beck, L.S. Katafygiotis, Updating robust reliability using structural test data, Probabilistic Eng. Mech. 16 (2001) 103–113.
[26] H. Jensen, C. Vergara, C. Papadimitriou, E. Millas, The use of updated robust reliability measures in stochastic dynamical systems, Comput. Methods Appl. Mech. Eng. 267 (2013) 293–317.
[27] D. Straub, I. Papaioannou, W. Betz, Bayesian analysis of rare events, J. Comput. Phys. 314 (2016) 538–556.

[28] D. Straub, I. Papaioannou, Bayesian updating with structural reliability methods, J Eng Mech. 141 (2015) 04014134.
[29] Y.S. Liu, L.Y. Li, Z.M. Chang, T. Yu, Reliability updating in the presence of distribution parameter uncertainty, 14th International Conference on Applications of Statistics and Probability in Civil Engineering, ICASP14, Dublin, Ireland, July 9-13, 2023.
[30] W.L. Fan, A.H.S. Ang, Z.L. Li, Reliability assessment of deteriorating structures using Bayesian updated probability density evolution method (PDEM), Struct. Saf. 65 (2017) 60–73.
[31] P.P. Li, L. Ren, Y.G. Zhao, Efficient method for updating the failure probability of a deteriorating structure without repeated reliability analyses, Struct. Saf. 102 (2023) 102314.
[32] R.Y. Rubinstein, D.P. Kroese, Simulation and the Monte Carlo method, John Wiley & Sons, 2016.
[33] P.T. Yuan, On the logarithmic frequency distribution and the semi-logarithmic correlation surface, Ann. Math. Stat. 4 (1933) 30–74.
[34] Y.M. Low, A new distribution for fitting four moments and its applications to reliability analysis, Struct. Saf. 42 (2013) 12–25.
[35] J. He, S.B. Gao, J.H. Gong, A sparse grid stochastic collocation method for structural reliability analysis, Struct. Saf. 51 (2014) 29–34.
[36] X. Jia, O. Sedehi, C. Papadimitriou, L.S. Katafygiotis, B. Moaveni, Hierarchical Bayesian modeling framework for model updating and robust predictions in structural dynamics using modal features, Mech. Syst. Signal Process. 170 (2022) 108784.
[37] A.-S. Ang, D. De Leon, Modeling and analysis of uncertainties for risk-informed decisions in infrastructures engineering, Struct. Infrastruct. Eng. 1 (2005) 19–31.
[38] Y.G. Zhao, Z.H. Lu, Structural reliability: approaches from perspectives of statistical moments, John Wiley & Sons, 2021.
[39] S.A. Smolyak, Quadrature and interpolation formulas for tensor products of certain classes of functions, Dokl Akad Nauk SSSR 148 (1963) 1042–1045.
[40] Z. Zhao, Z.H. Lu, Y.G. Zhao, An efficient extreme value moment method combining adaptive Kriging model for time-variant imprecise reliability analysis, Mech. Syst. Signal Process. 171 (2022) 108905.
[41] D. Xiu, J.S. Hesthaven, High-order collocation methods for differential equations with random inputs, SIAM J. Sci. Comput. 27 (2005) 1118–1139.
[42] Y.G. Zhao, T. Ono, New point estimates for probability moments, J. Eng. Mech. 126 (2000) 433–436.
[43] W. Betz, I. Papaioannou, D. Straub, Transitional Markov chain Monte Carlo: observations and improvements, J. Eng. Mech. 142 (2016) 04016016.
[44] R.X. Zhang, S. Mahadevan, Bayesian methodology for reliability model acceptance, Reliab. Eng. Syst. Saf. 80 (2003) 95–103.
[45] M. Ping, X. Han, C. Jiang, X. Xiao, A time-variant extreme-value event evolution method for time-variant reliability analysis, Mech. Syst. Signal Process. 130 (2019) 333–348.
[46] C. Andrieu-Renaud, B. Sudret, M. Lemaire, The PHI2 method: a way to compute time-variant reliability, Reliab. Eng. Syst. Saf. 84 (2004) 75–86.
[47] Y.G. Zhao, Y.Y. Weng, Z.H. Lu, An orthogonal normal transformation of correlated non-normal random variables for structural reliability, Probabilistic Eng. Mech. 64 (2021) 103130.
[48] A. Der Kiureghian, M.D. Stefano, Efficient algorithm for second-order reliability analysis, J. Eng. Mech. 117 (1991) 2904–2923.
[49] C. Dang, P.F. Wei, J.W. Song, M. Beer, Estimation of failure probability function under imprecise probabilities by active learning–augmented probabilistic integration, ASCE ASME J. Risk Uncertain. Eng. Syst. A Civ. Eng. 7 (2021) 04021054.